Ambipolar Diffusion of Photocarriers in Electrolyte–Filled, Nanoporous TiO 2 †

5 AUTHORS, INCLUDING:

Nikos Kopidakis
National Renewable Energy Laboratory, Gold…
117 PUBLICATIONS   5,563 CITATIONS

SEE PROFILE

Nam-Gyu Park
Sungkyunkwan University
222 PUBLICATIONS   10,861 CITATIONS

SEE PROFILE

Jao van de Lagemaat
National Renewable Energy Laboratory
104 PUBLICATIONS   6,326 CITATIONS

SEE PROFILE

Ambipolar Diffusion of Photocarriers in Electrolyte-Filled, Nanoporous TiO₂[†]

N. Kopidakis and E. A. Schiff*

Department of Physics, Syracuse University, Syracuse, New York 13244

N.-G. Park, J. van de Lagemaat, and A. J. Frank

National Renewable Energy Laboratory, Golden, Colorado 80401

Received: October 13, 1999

We report transient photocurrent measurements on solar cell structures based on dye-sensitized, porous TiO₂ films filled with a liquid electrolyte. The measurements are interpreted as ambipolar diffusion; under most measurement conditions, the ambipolar diffusion coefficient is dominated by electrons diffusing in the TiO₂ matrix. We report a strong dependence of the ambipolar diffusion coefficient upon the photoexcitation density, as has been proposed previously. The coefficients vary from 10^{-8} cm² s⁻¹ at low density to 10^{-4} cm² s⁻¹ for densities of 10^{18} cm⁻³. At a specified photoexcitation density, ambipolar diffusion coefficients measured using weak laser pulses and optical bias are about 10 times larger than coefficients measured using large-intensity laser pulses. We describe trapping models for these effects based on an exponential distribution ($T_0 = 650$ K) of electron trap levels in TiO₂. We infer an electron recombination cross section less than 2×10^{-27} cm²; this value is nearly 10 orders of magnitude smaller than typical values in compact semiconductors and indicates the extraordinarily effective separation of electrons in the TiO₂ matrix from electrolyte ions only nanometers distant.

Introduction

About 25 years ago, Harvey Scher and his collaborators Mel Lax and Elliott Montroll inaugurated the era of quantitative mobility measurements in highly disordered materials. In particular, they developed a convincing way—the continuous time random walk—of understanding charge carrier transport measurements in materials such as amorphous chalcogenides.[1,2] In such materials, a packet of carriers that is initially well-localized in space exhibits non-Gaussian dispersion as time passes—in remarkable contrast to essentially all previous transport measurements. Prior to the work of Scher and his colleagues, such dispersive transport had defied analysis. Our ability to understand this type of transport has proven invaluable as new materials such as hydrogenated amorphous silicon and organic semiconductors have risen to scientific and technological prominence beside the amorphous chalcogenides that launched electrophotography.

Porous electronic materials also exhibit dispersive transport. For such materials, the mechanism that causes the dispersion can be very different than that involved in compact amorphous semiconductors, and in particular, semiclassical carrier transport confined to random fractals is dispersive.[3] In the past decade, fundamental interest in transport on porous matrixes has been complemented by exciting prospects for technological applications, in particular by Canham's discovery that certain porous silicons can luminesce far more brightly than compact crystalline silicon[4] and by O'Regan and Grätzel's demonstration of a remarkably efficient photoelectrochemical solar cell based on dye-sensitized, nanoporous TiO₂.[5]

In this paper, we present transient photocurrent measurements on such porous TiO₂-based solar cells. In these cells, the pores of the TiO₂ matrix are filled with a liquid electrolyte, which profoundly alters the electrical processes. However, we first describe some previous work on unfilled porous TiO₂. Electron drift mobilities were recently measured in sintered anatase TiO₂ (20–30 nm diameter) by Dittrich et al.,[6] who inferred a drift mobility of 7×10^{-6} cm² V⁻¹ s⁻¹ near room temperature as well as a fairly strong temperature dependence. The mobility was independent of the electric field, indicating that electron transport was nondispersive. Its value is vastly lower than Hall mobility estimates for electrons in single-crystal anatase;[7] in common with many papers on electrical transport in nanoporous TiO₂, the decline was attributed to electron trapping, presumably by point defects. Somewhat earlier, Könenkamp et al.[8] reported that the electron drift mobility in nanoporous anatase TiO₂ could be improved by "filling" of these traps prior to the transient measurement.

The solar cells devised by O'Regan and Grätzel consist of a porous TiO₂ film prepared on a conducting substrate, stained by inorganic dyes that absorb visible illumination and then filled with a liquid electrolyte. A photon absorbed in a dye molecule leads to transfer of an electron into the TiO₂ and to a change of the charge state of a molecule in the electrolyte. Electrons then diffuse to the collecting substrate (macroscopic electric fields are screened by the electrolyte), and ionic counationcharge is collected by a top Pt electrode immersed into the electrolyte.[9]

The most direct previous measurement of photocarrier diffusion in electrolyte-filled cells was done by Solbrand et al.[10] Following absorption of an ultraviolet light pulse, they observed a photocurrent response pulse that was delayed from the optical pulse by a "transit time" τ_{TR}. They reported that this transit time scaled with thickness as $\tau_{TR} = L^2/D$ from which they

Ambipolar Diffusion of Photocarriers

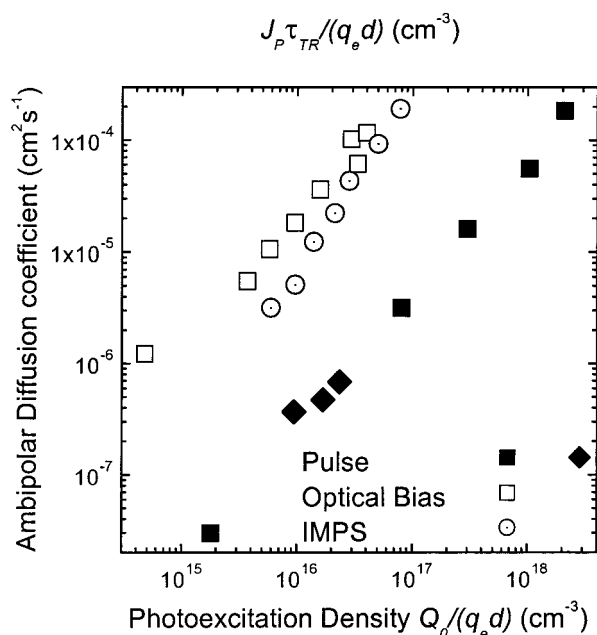*J. Phys. Chem. B, Vol. 104, No. 16, 2000* **3931**

Figure 1. Ambipolar diffusion coefficient D of photocarriers as a function of photoexcitation density N for dye-sensitized nanoporous TiO_2 solar cells. Pulse: from transient photocharge measurements with illumination pulses of varying strength ($N = Q_0/Aed$); results from two different samples are shown ($\blacksquare$, 7.0 μm; $\blacklozenge$, 7.5 μm). Optical bias: from transient photocharge measurements (7.0-μm sample) in the presence of bias light ($N = j_P\tau_{TR}/ed$). IMPS: from published measurements of intensity-modulated photocurrents in a similar sample.[16] Note that the diffusion coefficient is essentially proportional to N.

extracted a diffusion coefficient of 1.5×10^{-5} cm^2 s^{-1}; this experiment also implies nondispersive transport. A similar value (5×10^{-5} cm^2 s^{-1}) was inferred from published "intensity-modulated photocurrent spectroscopy" (IMPS) and photocurrent rise-time measurements by Dloczik et al.[11]

In the present paper, we present a series of transient photocurrent measurements on dye-sensitized nanoporous TiO_2 solar cells. Before outlining these measurements, however, we first note that we will use the concept of ambipolar diffusion and drift to interpret them. In these cells, there is strong electrostatic coupling of the motions of ions in the electrolyte and of electrons in the TiO_2 matrix. While this possibility is qualitatively acknowledged by a number of authors,[10-12] the well-established ambipolar diffusion model[13-15] has not been previously used for nanoporous TiO_2 cells, and it has not been noted that measurements determine ambipolar diffusion constants and ambipolar mobilities. Ambipolar diffusion permits a quantitative analysis of the interaction of electron and ion transport. For most cases, this analysis leads directly to the conclusion that electron diffusion within the TiO_2 matrix determines the dynamics of transient photocurrents. Fortunately, essentially the same conclusion was reached in previous work through different arguments. Nonetheless, a complete analysis of transient photocurrents is impossible without the ambipolar concept, and we return to this subject in the discussion section of this paper.

Our own transient photocurrent measurements were done over a wide dynamic range in time ($10^{-5}-10^2$ s), and they reveal an enormous variation in the ambipolar diffusion coefficient with the level of photoexcitation—from 3×10^{-8} to 10^{-4} cm^2 s^{-1}. In Figure 1, we summarize the ambipolar diffusion coefficient measurements as a function of the photoexcitation density for two types of photocurrent experiment with laser pulses. The "pulse" measurements were done simply using varying optical

intensities of the absorbed pulse. The "optical bias" measurements are the transient photocurrent response to a weak laser pulse in the presence of auxiliary illumination (optical bias). We also revisit some of our previous IMPS data on comparable samples.[16] As can be seen, the IMPS measurements are consistent with the optically biased transient measurements, as they must be, given the Fourier transform relation between them.[17]

Comparable IMPS measurements have been reported by several groups.[11,18-20] These measurements have not generally been reported in terms of intensity-dependent diffusion coefficients despite the common recognition of its possibility. In our subsequent discussion, we compare the previous estimates by other groups with those of Figure 1. The substantial difference in ambipolar diffusion coefficient for the large pulse and the optically biased pulse measurements has not (to our knowledge) been reported previously.

A strong dependence of the diffusion coefficient upon photoexcitation density may be roughly understood by the hypothesis of electron traps in the porous TiO_2 with a very broad distribution of release rates. Most authors have invoked this idea qualitatively; recently, there have been at least two efforts to infer exact level energy distributions for nanoporous TiO_2.[20,21] We perform a comparable analysis for the large pulse measurements near the end of this paper. While it is fairly straightforward to account for the dependence of diffusion coefficient upon photoexcitation density using an exponentially rising level energy distribution, we have not been able to account for the difference between the large pulse and the optically biased ambipolar diffusion constants using this approach.

Finally, we note how extraodinarily well-isolated the electrons in TiO_2 are from electrolyte ions only nanometers away: recombination coefficients are less than 2×10^{-20} cm^3 s^{-1}, corresponding to a "cross section" of less than 2×10^{-27} cm^2 under short-circuit conditions. This value is many orders of magnitude lower than "typical" values for compact semiconductors.

Experimental Methods

Preparation of Dye-Sensitized TiO$_2$ Solar Cells. Anatase TiO_2 slurries, consisting of 15–20-nm particles, were prepared by hydrolyzing titanium tetraisopropoxide (Aldrich, 99.999%) in the presence of distilled acetic acid followed by autoclaving at 230 °C for 12 h.[22] Conducting glass plates (1.2×1.25 cm; Asahi Glass Co.; F-doped SnO_2 overlayer, 80% transmittance in the visible, 5% haze, 10 Ω/square) were used as the substrate for depositing TiO_2 films. To control the thickness of the deposited films, a film casting knife (BYK-Gardner, AG-4341) was used. A drop of 10 mM titanium tetrabutoxide (Aldrich 99%) in 2-propanol was spread on the conducting glass surface to produce a thin layer of TiO_2 to isolate the conducting glass surface from the redox electrolyte.[23] The TiO_2 slurry was then spread on top of it. The TiO_2-covered glass was heated in air at 450 °C for 30 min and then allowed to cool. The thickness of the transparent films ranged from 1.5 to 12.5 μm, as measured with a Tencor Corp. Alpha-Step model mechanical profiler.

For photosensitization studies, the TiO_2 electrodes were immersed in acetonitrile/*tert*-butyl alcohol (50:50 v/v %) containing 3×10^{-4} M Ru[LL'(NCS)$_2$] (L = 2,2'-bipyridyl-4,4'-dicarboxylic acid, L' = 2,2'-bipyridyl-4,4'-ditetrabutyl-ammoniumcarboxylate) for 24 h at room temperature. The dye-covered electrodes were then rinsed with the acetonitrile/*tert*-butyl alcohol mixture and dried under an N$_2$ stream. To

minimize rehydration of TiO_2 from moisture in the ambient air, the electrodes were immersed in the dye solution while they were still warm (100−120 °C) from the annealing step.

Transparent Pt counter electrodes were prepared by spreading a drop of 5 mM hexachloroplatinic acid (Fluka, purum) in 2-propanol on the conducting glass followed by heating at 380 °C for 15 min in a hot air furnace.[24] The Pt electrode was placed over the dye-coated electrode, and the edges of the cell were sealed with 0.5-mm-wide strips of 25-μm-thick Surlyn (Dupont, grade 1702). Sealing was accomplished by pressing the two electrodes together at a pressure of 900 psi and a temperature of about 100 °C. The redox electrolyte consisted of 0.6 M 1,2-dimethyl-3-hexyl-imidazolium iodide and 40 mM I_2 in aceto-nitrile for the 7-μm-thick TiO_2 electrode and 0.8 M 1,2-dimethyl-3-hexyl-imidazolium iodide and 50 mM I_2 in methoxy acetonitrile (Fluka, purum) for all other electrodes (3.5-, 7.5-, and 12.5-μm-thick films). The redox electrolyte was introduced into the cell through one of two small holes drilled in the counter electrode. The holes were then covered and sealed with small squares of microscope objective glass and Surlyn. The edges of the cell were further sealed with low vapor-pressure epoxy (Varian, Inc. Torr Seal). The resulting cell had an active area of about 0.25 cm^2.

Transient Photocharge Measurements. The cells were illuminated with laser pulses, and the transient photocurrent response was recorded. The laser used was a nitrogen-laser pumped dye laser; the pulse duration was 3 ns, and the wavelength was typically 670 nm. At this particular wavelength, the absorption coefficient of the dye-sensitizer employed in those cells was low enough for a fairly uniform photocarrier density to be created throughout the volume of the thinner cells.

To obtain a wide range of pulse intensities, for some measurements the laser beam was focused into a spot significantly smaller than the area of the cell. Direct measurements of the beam profile were not performed, and we anticipate significant errors (at least a factor of 2) in intensity estimates. Some transient photocurrent measurements were made with continuous white bias light from a tungsten halogen (type ENH) bulb superimposed on the laser pulse.

The measurements were performed under short-circuit conditions, i.e., one electrode of the cell was grounded and the other was connected to a current preamplifier. Applying reverse bias voltages up to 200 mV to the cell did not change the shape of the photocurrent transients. The output of the current pre-amplifier was recorded by a digital oscilloscope with averaging capability. The rise-time of the signal was about 1 μs. Although we recorded transient photocurrents, for most analyses we show the transient photocharge obtained by numerical integration of the photocurrent.

Transient Photocharge Measurements

Thickness Dependence. Photocurrent transients for the three samples of different thicknesses are shown in Figure 2a. Illumination was through the top (Pt) electrode. The pulse intensity was the same for all three measurements. The time scale in Figure 2a starts at 3×10^{-5} s; the photocurrent reaches its maximum near 10^{-4} s. This early time behavior is most likely a consequence of the resistance−capacitance (RC) product of the capacitance of the cell (10 μF for all thicknesses) and the series resistance of the transparent conductive oxide (20 Ω).

Integrating the curves of Figure 2a in time, we obtain the total photocharge Q_0 generated in the cell. The results for the three different thicknesses are given in Table 1; for the two
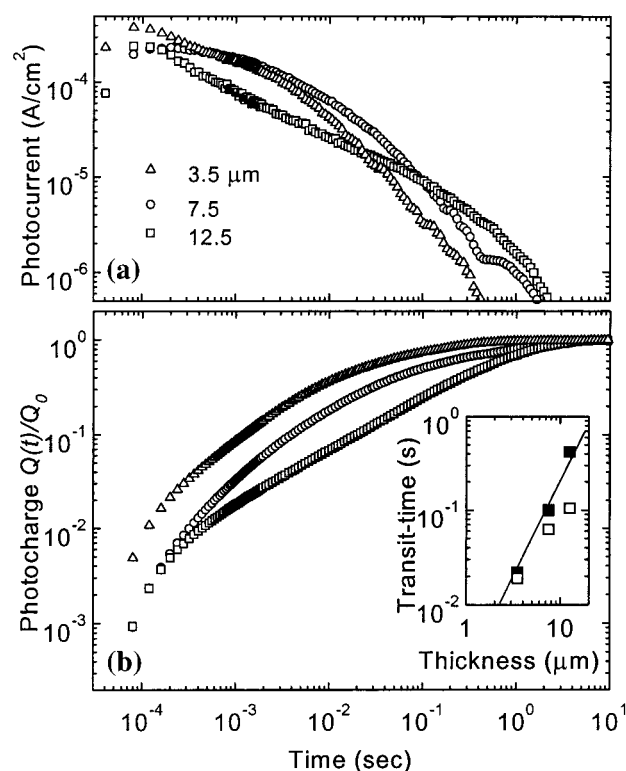

Figure 2. (a) Photocurrent transients for three samples of different thicknesses under illumination with 670-nm pulses though the semi-transparent Pt top electrode. The volume generation of photocarriers was approximately 4×10^{16} cm^{-3} for the pulse intensity used. The pulse intensity was kept the same for all samples. (b) Photocharge transients for the three different samples, calculated by numerical integration of the corresponding photocurrent curves (panel a). Curves are normalized by the maximum charge Q_0 reached at saturation. The value of Q_0 for each sample is given in Table 1. The inset shows the scaling of transit times of photocarriers with sample thickness. Solid symbols in the inset correspond to illumination through the semitrans-parent Pt top electrode, while open symbols correspond to illumination with the same pulse intensity through the TCO bottom electrode. The line demonstrates square dependence of transit time on thickness.

TABLE 1: Total Photocharge Q_0 Generated by a 670-nm Laser Pulse and the Average Photoexcitation Density N for Samples of Three Thicknesses (Top Illumination)

thickness (μm)	Q_0 ($\times 10^{-6}$ C/cm^2)	N ($\times 10^{16}$ cm^{-3})
3.5	2.5	4.4
7.5	6	5
12.5	6.8	3.4

thinner samples, Q_0 is proportional to thickness, indicating a uniform photocarrier density of about 5×10^{16} cm^{-3}. Q_0 increased very little for the thickest sample (12.5 μm), suggest-ing an absorption length at this wavelength comparable to the thickness.

For uniformly absorbed light and normal (Gaussian) diffusion, we expect the photocurrent to decay as the delay time $t^{-1/2}$, which is reasonably consistent with the decays in Figure 2. This power law can be understood from the following argument. At a time t after the laser pulse, those carriers photogenerated within a zone of width $(Dt)^{1/2}$ extending from the SnO_2/TiO_2 interface will have been collected: $Q(t) \propto t^{1/2}$. The corresponding photocurrent (the time derivative of $Q(t)$) decays as $t^{-1/2}$.

In Figure 2b, we present the transient photocharge $Q(t)$ obtained by integrating the photocurrent; to facilitate comparison of the varying thicknesses, we have normalized the three curves by the total photocharge Q_0. We now define a typical transit time for the collection of Q_0 as the time of half-collection τ_{TR}:

Ambipolar Diffusion of Photocarriers

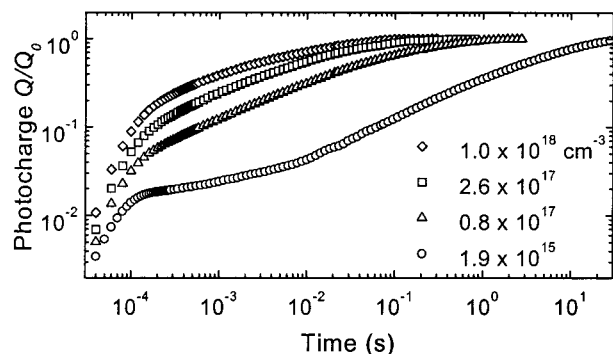*J. Phys. Chem. B, Vol. 104, No. 16, 2000* **3933**

Figure 3. Photocharge for the 7-μm-thick sample for four different laser pulse intensities. The corresponding volume generation of photocarriers, ρ, is given. Curves are normalized by the saturation photocharge Q_0.

$Q(\tau_{TR}) = Q_0/2$. In the inset to Figure 2b, we show the thickness dependence of this transit time; the solid and open symbols indicate illumination through the top and the substrate sides of the cell, respectively. The thickness dependence is reasonably consistent with the result expected for uniform illumination:

$$\tau_{TR} = \frac{(d/2)^2}{D} \quad (1)$$

The factor 1/2 on the thickness d allows for the fact that, under uniform illumination, about half the charge will have been collected when carriers have diffused half the thickness of the cell. Note that the results for illumination through the top and the substrate sides of the cell are consistent with this interpretation as well. For the thinnest sample, there is essentially no difference in transit times, which is consistent with precisely uniform photogeneration. As the samples get thicker and thicker, transit times for the top illuminated case exceed those for substrate illumination. For the thicker samples, photogeneration is mostly near the interface through which the sample is illuminated. Carriers generated with top illumination must diffuse a larger distance than those illuminated through the substrate.

Photoexcitation Density and Optical Bias Effects. Although the results in Figure 2 suggest that samples have a well-defined ambipolar diffusion coefficient D, we find a very strong dependence of these results upon the photoexcitation density involved in the measurement. In Figure 3, we illustrate this effect on the photocharge transients for the 7-μm-thick sample. Once again, the photocharge curves are normalized by their saturation value Q_0 at long times. Note that, for very low photoexcitation densities, the photocharge deviates substantially from the rough $t^{1/2}$ form found at higher intensities. We discuss the form for these transients in more detail subsequently.

A summary of the total photocharge measurements for the 7-μm sample with varying pulse intensity is shown in Figure 4. Note that Q_0 scales with pulse intensity. Transit times decline approximately as $(Q_0)^{-1}$.

As shown in the above results, linear response is not achieved in these measurements, since transit times depend on pulse intensity over the entire range spanned by our laser pulses. We thus explored the other extreme, i.e., increasing the photocarrier density in the sample by illumination with continuous white light, which we hereafter call bias light. In this experiment, the bias light establishes a DC photocurrent, which is perturbed by the additional photocarrier density created by the laser pulse.

The low pulse intensity was kept fixed, while the bias light intensity was varied to measure the family of photocharge curves
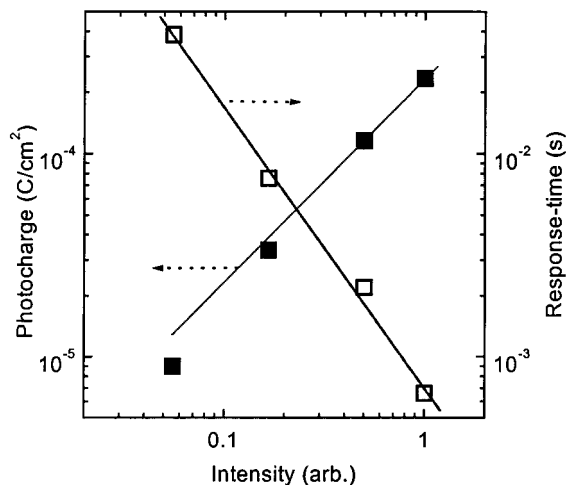

Figure 4. Dependence of the photocharge Q_0 and response time upon laser pulse intensity. Photocharge scales essentially linearly with pulse intensity; the response time falls somewhat faster than inversely with intensity.
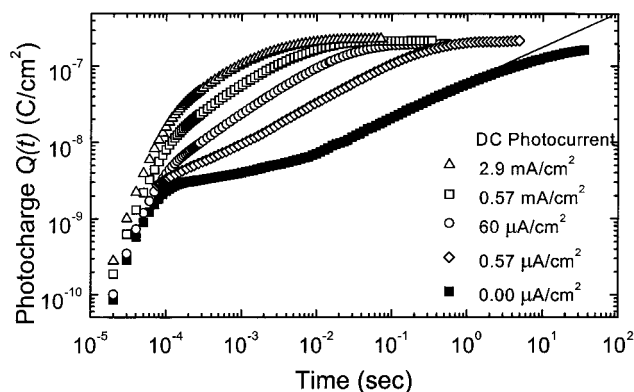

Figure 5. Photocharge transients under white bias light. The photocurrent density induced by the bias light is shown for each curve. The solid symbols correspond to a measurement without bias light. The laser pulse intensity was the same for all curves.

shown in Figure 5. Note that the curves of Figure 5 are not normalized and that the value of charge reached at saturation is almost independent of bias light intensity. We verified that, under bias light, photocharge transients were proportional to pulse intensity.

Discussion

Ambipolar and Electron Diffusion. Ambipolar diffusion typically occurs when a electrical carrier is injected into a sea of oppositely charged, mobile carriers; under these conditions, the injected charge is referred to as a minority carrier. In homogeneous semiconductors, the classic case is the photogeneration of electrons in a *p*-type material with a large equilibrium concentration of holes. In highly conductive media such as doped semiconductors, there can be only very modest deviations from electrical neutrality; such deviations occur on the Debye length scale $L_D = (k_B T \epsilon \epsilon_0 / ep)^{1/2}$ where p is the hole density, e is the electronic charge, k_B is the Boltzmann's constant, and $\epsilon \epsilon_0$ is the dielectric constant. Over larger length scales, space-charge neutrality is maintained, so the separate diffusion or the drift of electrons and holes must be constrained so that no net space charge is created. Mathematical treatment of this case has been done many times in reviews and textbooks,[15,25,26] and we simply reproduce the standard result

for the ambipolar diffusion coefficient:

$$D_{amb} = \frac{(n + p)}{(n/D_p) + (p/D_n)} \qquad (2)$$

where n and D_n are the electron density and diffusion coefficient, respectively, and p and D_p are the hole density and diffusion coefficient. As can be seen by inspection, if the density of holes p vastly exceeds the density of electrons n, $D_{amb} = D_n$; this conclusion applies even when the holes are substantially less mobile than the electrons. Thus a "packet" of excess minority carriers generated by light or by contact injection will diffuse naturally, carrying along with it a cloud of holes so that the entire packet remains electrically neutral.

The ambipolar diffusion model leads directly to the conclusion that electron diffusion confined to the TiO$_2$ matrix determines the dynamics of transient photocurrents in electrolyte-filled cells. The ambipolar model undoubtedly applies: we estimate a Debye length for the electrolye of about 0.1 nm. The concentration of ions in a 0.5 M electrolyte solution is about 3 $\times$ 10^{20} cm^{-3}. For the purpose of illustration, we assume an ion diffusion coefficient of 10^{-5} cm^2 s^{-1}. The largest photoexcitation density used in our experiments was about 2 $\times$ 10^{18} cm^{-3}, and the corresponding ambipolar diffusion coefficient under large pulse conditions was 2 $\times$ 10^{-4} cm^2 s^{-1}. Substitution of these values into eq 2 yields $D_n = 2.29 \times 10^{-4}$ cm^2 s^{-1}. There is thus about a 15% difference between the measured ambipolar diffusion coefficient and the electron diffusion coefficient under the highest excitation conditions; as n diminishes, the equality of the ambipolar and electron values becomes essentially exact.

This same conclusion, that electron diffusion dominates transient photocurrents in electrolyte-filled nanoporous TiO$_2$ cells, has been reached by most earlier workers using quite different arguments. In particular, intensity-dependent diffusion coefficients and odd frequency dependences in IMPS measurements are far more likely to reflect electron trapping by the solid-state system than to reflect electrolyte effects. Another approach is to prove the independence of the transient photocurrents upon electrolyte properties, and in one experiment, the electrolyte viscosity (and hence the ionic diffusion coefficients) was varied, with little effect on the photocurrents.[27] On the other hand, Solbrand et al.[10] found at least a 5-fold decline of the ambipolar diffusion coefficient as the molarity of their electrolyte was reduced from 500 to 20 mM. This latter result may be explicable as the crossover from the electron to the ion-dominated value for the ambipolar diffusion coefficient (cf. eq 2) as the ion density declines, and in any event, this analysis shows the value of the ambipolar diffusion expression.

In the Appendix, we further outline the relationship between previous mathematical models for photocurrents in electrolyte-filled TiO$_2$ and the ambipolar diffusion model; remarkably, most treatments have converged to equations that are fairly consistent with ambipolar diffusion.

Summary of Diffusion Coefficients. In Figure 1, we summarize the ambipolar diffusion coefficient estimated from both the large pulse and the optical bias experiments as a function of photoexcitation density. We estimated the photoexcitation density due to optical bias using the approximation:

$$N \approx j_{DC}\tau_{TR}/ed \qquad (3)$$

Although both measurements reveal a comparable dependence upon photoexcitation density, there is plainly a substantial difference in magnitude.

The difference between the two measurements is presumably affected by the different nonuniformities in the photoexcitation density for the steady-state and the large pulse experiment; this effect may be significant because of the large influence of photoexcitation density upon ambipolar diffusion. We have not made calculations to test this mechanism, but it seems unlikely to account for the nearly 10-fold difference in diffusion coefficients. We return to this subject briefly at the end of the section on trapping models.

In Figure 1, we have also included estimates based on the IMPS measurements of Schlichthörl et al.[16] for which we believe the sample to be quite similar to those studied here. We analyzed these data by extracting an intensity-dependent time constant τ_{imps} from the frequency dependence of the measurements. One would expect this procedure to give results close to the transit time we have employed for the present measurements with laser pulse, and indeed the IMPS data are quite comparable with the optically biased transient measurements.

We first compare electron drift-mobility measurements in nanoporous TiO$_2$ (without an electrolyte)[6,8] to the present measurements using laser pulses alone (without optical bias). Dittrich et al.[6] reported an electron drift mobility of 7 $\times$ 10^{-6} cm^2 V^{-1} s^{-1} at 300 K, corresponding to $D = 2 \times 10^{-7}$ cm^2 s^{-1}. We calculate from their paper that this estimate corresponds to a photoexcitation density at the transit time of 3 $\times$ 10^{17} cm^{-3}. Inspecting Figure 1, we find that this value is about 100 times smaller than we obtained in an electrolyte-filled cell. The results of Solbrand et al.[10] may also be compared with the "pulse" data of Figure 1. The authors reported a diffusion coefficient of 1.5 $\times$ 10^{-5} cm^2 s^{-1} with 700 mM electrolyte strength. For their thickest sample, we estimate that this coefficient corresponds to a mean photoexcitation density N of about 10^{17} cm^{-3} at the transit time (when excitation conditions are most uniform). For their thinnest sample, $N \approx 10^{18}$ cm^{-3}. The magnitude of their measurements is thus in very rough agreement with those of Figure 1, although their data do not seem to exhibit the anticipated dependence upon N.

The diffusion coefficients in the present work agree well with the results of Cao et al.;[19] an appropriate replotting of their IMPS time-constant measurements overlaps the optical bias and the IMPS data of Figure 1. Dloczik et al.[11] did not provide sufficient information for us to compare the magnitude of their diffusion coefficients with those of Figure 1.

Absence of Recombination. Our measurements of temperature dependence and bias light dependence of photocharge show that the total photocharge reached at saturation is independent of bias light intensity and temperature. This indicates that there is no significant recombination of photocarriers in our measurements. This observation is striking to us. Transit times of photoelectrons are as long as a few seconds for the lowest pulse intensities, but still there is no significant recombination observed. We can use these measurements to infer the coefficient $b = R/N_I$ governing the recombination rate R of an electron within the TiO$_2$ matrix with ions of density N_I in the electrolyte. Under weak illumination, the recombination rate $R < 0.5$ s^{-1}, and the density of iodine ions is about 3 $\times$ 10^{19} cm^{-3}. We obtain $b < 1.5 \times 10^{-20}$ cm^3 s^{-1}. The amazingly small magnitude may be better understood if converted to a conventional recombination cross section $\sigma = b/v_{thermal}$, where $v_{thermal}$ is a conventional thermal velocity of the order 10^7 cm s^{-1}. We obtain $\sigma < 1.5 \times 10^{-27}$ cm^2, which is around 10 orders of magnitude lower than is typical for compact semiconductors. Such weak recombination is clearly at the heart of the successful solar cells based on porous TiO$_2$.

Ambipolar Diffusion of Photocarriers

J. Phys. Chem. B, Vol. 104, No. 16, 2000 **3935**

Trapping Models. The values of D in Figure 1 are much lower than the value of 10^{-1} cm^2 s^{-1} that may be estimated by using the Einstein relation from Hall effect mobilities for electrons in single-crystal anatase[7] TiO$_2$. There are at least two plausible explanations for this reduction. First, defects in the porous TiO$_2$ may act as electron traps, immobilizing and later releasing electrons. Several authors have interpreted photocurrent measurements in TiO$_2$ in terms of various distributions of trap states. Second, an intrinsic reduction in mobility (or diffusion) due only to the porous geometry may also occur. This mechanism has been clearly observed for electron photocarrier mobilities of porous Si.[28]

The decrease in transit times with increasing photoexcitation density in the TiO$_2$ is readily explained using an exponentially rising level-energy distribution $g(E)$ of traps. There is a long history for this model, dating at least to the work of Rose in the 1950s;[29] Tiedje has reviewed the model's predictions for transient measurements.[30] Here, we give the appropriate variation of earlier work[31] for the absorption of strong pulse of illumination. A very different treatment of the model, including applications to phenomena not treated here, has been given recently by Nelson.[21] We write the exponential distribution of traps as

$$g(E) = g_0 \exp\{-(E_C - E)/kT_0\} \quad (4)$$

where E is an electron level energy, E_C denotes the energy level (the transport edge) that divides states in which the electrons are mobile from states in which electrons are trapped, and g_0 and kT_0 are parameters of the exponential distribution. In homogeneous, crystalline materials, the transport edge may be identified with the edge of the conduction band; such an identification is neither necessary nor desirable for disordered materials.

The trap occupancy $f(E)$ prior to absorption of the laser pulse is assumed negligible. We consider the behavior $f(E,t)$ for uniform absorption. We initially neglect carrier loss to the electrodes, which of course becomes significant at the transit time τ_{TR}. While $f(E,t)$ is rather complex in general,[31] for fairly broad conditions $f(E)$ will ultimately (after a "complete thermalization time" τ_T) correspond to a Fermi distribution that simply fills deeper-lying states up to a quasi-Fermi energy E_{fn}. Assuming for simplicity that the exponential form for the density of states extends to the transport edge, we then obtain the following expressions governing the density n of mobile electrons and the total density N of electrons photogenerated by the pulse:

$$n = N_C \exp\{-(E_C - E_{fn})/kT\}$$

$$N = (N_C/A) \exp\{-(E_C - E_{fn})/kT_0\}$$

$$A = [(T/T_0)^2 \pi/\sin((T/T_0)\pi)]$$

$$n = AN_C(N/N_C)^{T_0/T} \quad (5)$$

Here $N_C = kTg_0$ is the effective density of states at the transport edge; the parameter A is nearly unity and is usually neglected in practical use. These expressions are valid at times $\tau_T < t$ sufficiently long for the simple trap-filling view to be valid and apply up to the transit time τ_{TR} (corresponding to 50% collection of the total photocharge). The diffusion coefficient obtained from transit times is thus

$$D = D_0 \frac{n}{N} = AD_0(N/N_C)^{(T_0/T)-1} \quad (6)$$

where D_0 is the diffusion coefficient for mobile electrons (above the transport edge and unaffected by trapping).[32]

The measurements in Figure 1 (pulsed excitation) exhibit the power law relation predicted by eq 6, and we obtain an estimate for $T_0 = 650$ K. The present model also provides a reasonable explanation for the behavior of the photocharge transients for very low excitation densities (solid symbols in Figure 5, $N \approx 2 \times 10^{15}$ cm^{-3}). The "kink" observed at about 10^{-2} s, where the photocharge begins to rise noticeably above a plateau value near 5×10^{-9} C/cm^2, may be identified with the time t_T required for the photocarrier distribution to relax to the Fermi distribution, as assumed by the derivation above. Using the approximation $E_C - E_{fn} \approx kT \ln(\nu t_T)$ and using a conventional value $\nu = 10^{12}$ s^{-1}, we infer a quasi-Fermi energy position 0.58 eV below the transport edge at this photoexcitation density.

Essentially the same eq 6 applies for optically biased transients (or IMPS),[17] where the photoexcitation density N must be redefined as that produced by the steady-state illumination. As can be seen from Figure 1, the value for T_0 from these data is comparable, but the quantitative difference in D for the two measurements (at a given photoexcitation density) is unexplained. We have also made a preliminary analysis of modulated photovoltage measurements by Schlichthörl et al.[20], which yielded a larger value $T_0 = 1160$ K. We therefore emphasize the preliminary character of the models based on trap level-energy distributions.

Conclusions

We have reported measurements of the ambipolar diffusion coefficient in TiO$_2$-based nanocrystalline solar cells. We identify electrons diffusing in the TiO$_2$ matrix as the minority carriers that determine D; because of the very much larger density of ions in the electrolyte, the ionic mobility is unimportant. The value of the electron diffusion coefficient depends strongly upon the optical excitation density. We report values for D as low as 3×10^{-8} cm^2 s^{-1} at very low light intensities and rising to 10^{-4} cm^2 s^{-1} for the highest intensity used. For constant photoexcitation density, diffusion coefficients measured using a laser pulse under optical bias are about 10 times larger than coefficients measured using large-intensity pulses alone.

Appendix

We comment in general on the implications of ambipolar transport for previous mathematical modeling of photocurrents in electrolyte-filled nanoporous TiO$_2$ cells.

Photocurrents and Displacement Currents. Previous modeling for electrolyte-filled cells has typically stated that the area-normalized transient photocurrent $I(t)/A$ measured in the electrical bias circuit can be equated to the electrical current density $j(x,t)$ within the sample evaluated at a boundary such as the substrate interface. This assumption is not valid for transients. The electrical current $I(t)$ flowing in the bias circuit are those required to maintain the electric potential difference across the

electrodes, and in particular transient photocurrents must be obtained by analyzing the displacement current $j_D = \epsilon\epsilon_0[\partial E(x,t)/\partial t]$ arising from the time-dependent electric fields between the two electrodes. The displacement current effect may be handled by spatial integration of the electrical current density:[33]

$$\frac{I(t)}{A} = \frac{\int_0^L j(x,t)\,dx}{L} \tag{7}$$

As an example, the drift-mobility measurements on nanoporous TiO$_2$ without an electrolyte are displacement current detected, as indeed are most drift-mobility measurements in low-mobility materials.

In electrolyte-filled cells, displacement currents from the bulk of the device may be negligible, since the electric field in this region is typically negligible. Under these ambipolar transport conditions, where displacement currents are confined to very small regions near the electrodes, the measured transient photocurrent may be more simply evaluated in terms of the extraction of electrons at the electrolyte/substrate barrier. There is a close analogy to the Haynes−Shockley experiment, which was probably the first time-of-flight determination of carrier mobilities in semiconductors.[34] This experiment measured ambipolar drift in *p*-type crystalline Ge by extracting electrons with a point-contact and measuring the time-of-flight between their generation at one point and their extraction. Thus, diffusion and drift-mobility measurements under ambipolar conditions are based upon arrival time detection. A simple theorem connects arrival time detected signals with uniform photogeneration to displacement current detected signals with surface illumination.[35]

In summary, the equation of the transient photocurrent in the external bias circuit to an interfacial electrical current density, as done by several authors, is valid only when the bulk of the device operates under ambipolar conditions.

Inseparability of Electron and Ion Motions. Previous mathematical treatments of photocarrier processes in the bulk of electrolyte-filled TiO$_2$ cells have not explicitly coupled electron and ion motion, thus suggesting the possibility of separable electron and ion motion. Transient photocurrents have generally been modeled by considering electron diffusion processes as if these were independent of electrolyte ions. Since it appears that ambipolar diffusion is electron-dominated under most conditions, this treatment can yield correct results. However, suggestions that portions of the transients are due to separate processes involving ion diffusion in the bulk of the cell are erroneous, as are any models leading to space charges in the bulk of the electrolyte-filled cells.

References and Notes

(1) Scher, H.; Lax, M. *Phys. Rev. B* **1973**, *7*, 4502.

(2) Scher, H.; Montroll, E. *Phys. Rev. B* **1975**, *12*, 2455.

(3) *Fractals and Disordered Systems*; Bunde, A., Havlin, S., Eds.; Springer: Berlin, 1996.

(4) Canham, L. *Appl. Phys. Lett.* **1990**, *57*, 1046.

(5) O'Regan, B.; Grätzel, M. *Nature* **1991**, *353*, 737.

(6) Dittrich, Th.; Lebedev, E. A.; Weidmann, J. *Phys. Status Solidi A* **1998**, *R5*, 165.

(7) Forro, L.; Chauvet, O.; Emin, A.; Zuppiroli, L.; Berger, H.; Levy, F. *J. Appl. Phys.* **1994**, *75*, 633.

(8) Könenkamp, R.; Hoyer, P.; Wahl, A. *J. Appl. Phys.* **1996**, *79*, 7029.

(9) Zaban, A.; Meier, A.; Gregg, B. A. *J. Phys. Chem. B* **1997**, *101*, 7985.

(10) Solbrand, A.; Lindström, H.; Rensmo, H.; Hagfeldt, A.; Lindquist, S.-E. *J. Phys. Chem. B* **1997**, *101*, 2514.

(11) Dloczik, L.; Ileperuma, O.; Lauermann, I.; Peter, L. M.; Ponomarev, E. A.; Redmond, G.; Shaw, N. J.; Uhlendorf, I. *J. Phys. Chem. B* **1997**, *101*, 10281.

(12) Schwarzburg, K.; Willig, F. *J. Phys. Chem. B* **1999**, *103*, 5743.

(13) van Roosbroeck, W. *Phys. Rev.* **1953**, *91*, 282.

(14) Scales, J. L.; Ward, A. L. *J. Appl. Phys.* **1968**, *39*, 1692.

(15) Dolezalek, F. K. In *Photoconductivity and Related Phenomena*; Mort, J., Pai, D. M., Eds.; Elsevier: Amsterdam, 1976; p 27.

(16) Schlichthörl, G.; Park, N. G.; Frank, A. J. *J. Phys. Chem. B* **1999**, *103*, 782.

(17) The intensity-modulated photocurrent may be viewed as the Fourier transform of transient photocurrent measurements in the presence of steady-state illumination (optical bias). Pandya, R.; Schiff, E. A. *Philos. Mag. B* **1985**, *52*, 1075.

(18) de Jongh, P. E.; Vanmaekelbergh, D. *Phys. Rev. Lett.* **1996**, *77*, 3427; *J. Phys. Chem. B* **1996**, *101*, 2716.

(19) Cao, F.; Oskam, G.; Meyer, G. J.; Searson, P. C. *J. Phys. Chem. B.* **1996**, *100*, 17021.

(20) Schlichthörl, G.; Huang, S. Y.; Sprague, J.; Frank, A. J. *J. Phys. Chem. B* **1997**, *101*, 8141.

(21) Nelson, J. *Phys. Rev. B* **1999**, *59*, 15374.

(22) Zaban, A.; Ferrere, S.; Sprague, J.; Gregg, B. A. *J. Phys. Chem. B* **1997**, *101*, 55.

(23) Smestad, G. *Sol. Energy Mater. Sol. Cells* **1994**, *32*, 273.

(24) Papageorgiou, N.; Maier, W. F.; Grätzel, M. *J. Electrochem. Soc.* **1997**, *144*, 876.

(25) Sze, S. M. *Physics of Semiconductor Devices*, 2nd ed.; Wiley: New York, 1981.

(26) Seeger, K. *Semiconductor Physics: An Introduction*, 5th ed.; Springer-Verlag: Berlin, 1991.

(27) Sommeling, P. M.; Rieffe, H. C.; Kroon, J. M.; van Roosmalen, J. A. M.; Schönecker, A.; Sinke, W. S. Spectral Response and Response Time of Nanocrystalline Dye-Sensitized TiO$_2$ Solar Cells. Presented at the 14th European Photovoltaic Solar Energy Conference, 1997.

(28) Rao, P. N.; Schiff, E. A.; Tsybeskov, L.; Fauchet, P. In *Advances in Microcrystalline and Nanocrystalline Semiconductors*; Materials Research Society, Symposium Proceedings: Pittsburgh, 1997; Vol. 452, p 613.

(29) Rose, A. *Photoconductivity and Allied Topics*; Wiley: New York, 1962; reprinted Krieger: Malabar, FL, 1978.

(30) Tiedje, T. collected in Joannopoulos, J. D.; Lucovsky, G. *Hydrogenated Amorphous Silicon II*; Springer: New York, 1984; pp 261−300.

(31) Schiff, E. A. *Phys. Rev. B* **1981**, *24*, 6189.

(32) Note that the prior treatments of the exponential bandtail model are mostly concerned with carrier mobilities and not with diffusion. The generalized Einstein relation suggests that mobilities and diffusion coefficients are simply proportional even including trapping effects; recent references include (a) Gu, Q.; Schiff, E. A.; Grebner, S.; Wang, F.; Schwarz, R. *Phys. Rev. Lett.* **1996**, *76*, 3196. (b) Metzler, R.; Barkai, E.; Klafter, J. *Phys. Rev. Lett.* **1999**, *82*, 3563.

(33) Scher, H. In *Photoconductivity and Related Phenomena*; Mort, J., Pai, D. M., Eds.; Elsevier: Amsterdam, 1976; p 92.

(34) Haynes, J. R.; Shockley, W. *Phys. Rev.* **1951**, *81*, 835.

(35) Schiff, E. A.; Parker, M. A. *Phys. Rev. Lett.* **1988**, *60*, 1454.